RSC Advances

ROYAL SOCIETY OF CHEMISTRY

www.rsc.org/advances

Cross-linked PS-DVB/Fe_3O_4 microspheres with quaternary ammonium groups and application in removal of nitrate from water

Zhenliang Feng[1], Wenrui Wei[1], Litong Wang[1], Ruoyu Hong[1, 2*]

[1.] School of Chemical Engineering, Fuzhou University, Fuzhou 350108, China

[2.] College of Chemistry, Chemical Engineering and Materials Science & Key Laboratory of Organic Synthesis of Jiangsu Province, Soochow University, SIP, Suzhou 215123, China

Abstract: Cross-linked PS-DVB/Fe_3O_4 microspheres (PFM-3) have been successfully synthesized by a new magnetic colloid swelling polymerization method and further functioned by alternatively using methylamine and 1, 4-butanediol diglycidyl as monomers to build a branching polymer with quaternary ammonium groups. The characterization of PFM has been performed by XRD, FT-IR, SEM, TEM and BET surface area analyses. The results showed that PFM-3 possessed high ion adsorption capacity (149.25 mg/g) which could adsorb nitrate ion from water efficiently and the material also showed excellent reusability (after washing with sodium chloride, the absorption capacity was little reduced). More important, the magnetic microspheres could be removed from waste water easily via introducing an external magnetic field, which made the discoveries in this study provide an effective and environmentally friendly approach for fast removal of nitrate from waste water.

Keywords: magnetic, PS-DVB/Fe_3O_4 microspheres, quaternary ammonium groups, nitrate removal

*Corresponding author. Tel: +86-512-6588 2057; Fax: +86-512-6588 2057. E-mail: rhong@suda.edu.cn

1. Introduction

Due to the high solubility, nitrate contamination is widely dissolved in surface and ground water.[1] Nitrate will threat the health of humans and animals as it is proved to be toxic, which could result in many diseases, such as birth defects, spontaneous abortion, increased infant mortality, diarrhea, abdominal pain, vomiting, diabetes, hypertension, respiratory tract infections, changes in the immune system, and methemoglobinemia.[2-7] Increased industrial and agricultural activities have resulted in the generation of toxic pollutants, and when their infiltrated into ground, the concentration of nitrate in ground water would be significantly increased.[8-10] Hence, nitrate removal from waste water is essential in the present scenario.

How to remove nitrate from water efficiently remains one of the most challenged topics. Studies like ion exchange, biological denitrification, reverse osmosis and electrodialysis etc. have been widely conducted.[11-17] Biological denitrification method using degradation of microorganism offers the possibility of a very specific and selective reduction of nitrate to nitrogen. However, there are some limitations due to contamination of drinking water with germs and metabolic substances which is still necessary to extensively recondition by filtration and germicidal treatment.[16] Ion exchange technology is identified as a more suitable technology for water decontamination and removal of inorganic ions due to its simplicity, effectiveness, selectivity, recovery and relatively low cost.[16-18] Therefore, researches on novel adsorbents based on ion exchange technology are attracting the global concern considering practical application. As known to all, macroporous

styrene-divinylbenzene copolymer has always been employed as the host material due to its satisfactory mechanical strength and easy chemical modification.[19] For example, Song et al. used macroporous styrene-divinylbenzene as host material after chloromethylation and following quaternarization to synthetize NDP-2 resin.[20] Although those materials have achieved expected functions in selective removal of nitrate from water and demonstrate a more preferable absorption of nitrate ion towards other anions, such as SO_4^{2-}, Cl^- and HCO_3^-, there still exists some disadvantages, such as difficulty in collection. Recently, since magnetic materials can be easily separated from the water efficiently via introducing an external magnetic field, the applications of magnetic materials in water treatment fields, such as heavy metal ion adsorption,[21-23] removal of organic contaminants,[24-27] and oil spill recovery,[28-31] have attracted increasing attention in decades. For example, Mao et al. synthetized the magnetic P(St-DVB)/Fe_3O_4 microspheres with hollow and porous structure for fast and selective absorption of oils from water surface. And the oil-absorbed microspheres could be removed from water surface efficiently via introducing an external magnetic field.[32] However, the magnetic material with quaternary ammonium groups for the adsorption of anions has seldom been reported before.

In this study, magnetic PS-DVB/Fe_3O_4 microspheres functioning as strong basic anion exchange resin were fabricated by a magnetic colloid swelling polymerization process and further functioned by alternatively using methylamine and 1, 4-butanediol diglycidyl as monomers to build a branching polymer with quaternary ammonium

groups. The effect of pH on the ion exchange ability and the reusability of PFM had been studied. The equilibrium adsorption isotherms of nitrate onto PFM were also investigated. Both Langmuir and Freundlich equations could be used to fit the equilibrium isotherms well.

2. Experimental

2.1 Materials

All chemicals were analytic reagent grade and used without further treatment, and all solutions were prepared with deionized water. Iron (III) chloride hexahydrate ($FeCl_3$•$6H_2O$), iron (II) sulfate heptahydrate ($FeSO_4$•$7H_2O$), aqueous ammonia (25%), azobisisobutyronitrile (AIBN), oleic acid, potassium persulfate (KPS) and sodium dodecyl sulfate (SDS) were received from Sinopharm Chemical Reagent Co. Ltd. (Shanghai, China). Styrene (St), divinylbenzene (DVB) (80 %), glycidyl methacrylate (GMA), methylamine (MA, 40% in H_2O, v/v) and 1, 4-butanediol diglycidyl ether (BDDE, 60%in H_2O, v/v) were bought from Aladdin Chemical Co. (Shanghai, China).

2.2. Preparation of lipophilic magnetic Fe_3O_4 nanoparticles

The preparation of lipophilic magnetic Fe_3O_4 nanoparticles included two steps: firstly, magnetic Fe_3O_4 nanoparticles were synthesized by means of co-precipitation method. $FeCl_3$•$6H_2O$ and $FeSO_4$•$7H_2O$ were dissolved in deionized water according to a molar ratio of 3:2 and put into a flask under nitrogen protection. After stirring for an hour, aqueous ammonia (25%) was quickly added into the solution. Keep the temperature at 80 °C for an hour, and then the pure magnetite particles were prepared.

Secondly, oleic acid was added into the above solution. Keep stirring for another hour under 80 °C, and then the lipophilic magnetic Fe_3O_4 nanoparticles were prepared.

2.3 Preparation of PS-DVB/Fe_3O_4 microspheres

PS-DVB/Fe_3O_4 microspheres were prepared by magnetic colloid swelling polymerization method. In the experiment, 200 mL deionized water and 5 g self-made hydrophobic magnetic Fe_3O_4 nanoparticles were added in a 500 mL three-necked round bottom flask under nitrogen protection. Then, 5 mL styrene and 0.5mL DVB were dispersed into the above solution. After stirring (200 rpm) for an hour and when the temperature reached at 70 °C, 0.1 g AIBN was added in and then the polymerization process started. Keep stirring for 10 hours, and then the PS-DVB/Fe_3O_4 microspheres were prepared. The resulting magnetic polymeric microspheres were magnetically separated after the addition of ethanol and washed for 5 times with 50 mL of ethanol, and then dried in vacuum oven at 60 °C for 24 h. The resulting microspheres were marked as PS-DVB/Fe_3O_4 particles.

2.4 Modified PS-DVB/ Fe_3O_4 microspheres with GMA.

5 g PS-DVB/Fe_3O_4 microspheres and 1mL GMA were dispersed in 200 mL ethanol. After stirring for 1 hour under nitrogen protection, 10 mL ethanol solution with 0.1 g SDS was slow added into the above solution, then kept the solution under 70 °C with stirring (200 rpm) for 24 hours. After the reaction completed, the resulting magnetic polymeric microspheres were magnetically separated after the addition of ethanol, and then washed 5 times with 50 mL of ethanol, and finally dried in vacuum oven at 60 °C for 24 h.

2.5. Synthesis of PFM

GMA modified PS-DVB/Fe_3O_4 microspheres were quaternary ammonium modified by a multi-step synthesis process. The basic condensation polymerization chemistry depended on MA and BDDE as monomers to build a branching polymer that has quaternary ammonium groups. 500 mg GMA modified PS-DVB/Fe_3O_4 was added into 20 mL MA (4%, v/v) and heated to 65 °C for 30 min; next 20 mL BDDE (10%, v/v) was added to the above solution and heated to 65 °C for 30 min. In each step, the brown solid was magnetically separated and rinsed with deionized water. The final two steps were repeated 1, 2 and 3 times to make 2, 3 and 4 layers of polymer on PFM, respectively. After being washed three times with 50 mL of 0.6 M NaCl solution and dried in vacuum oven at 60 °C for 24 h, the PFM with different numbers of bonded layers and positive charge were obtained.

2.6. Batch adsorption experiments

Batch adsorption experiments were carried out in 150 mL conical flasks according to the detailed experimental procedure described by Milmile and Chen et al. [1, 33] The PFM (0.1 g) was contacted with nitrate in solution (50 mL) with different concentrations (50, 100, 200, 400 and 600 mg/L, respectively) for adsorption isotherm study at 293 K separately. The flasks were then transferred to an incubator shaker and vibrated at 140 rpm for 24 h to ensure the equilibrium adsorption. The effect of pH on the ion exchange ability and the reusability of PFM were also studied. All batch experiments were repeated for at least three times under the same conditions and all the data appeared in this article were the average value.

2.7. Characterization

Fourier transformation infrared (FT-IR) spectroscopy was carried out using the potassium bromide (KBr) disk method by a Nicolet Avatar 360 Fourier transform infrared spectrometer to analyze a series of products in the process of synthetizing PFM. The structure of a series of products was investigated by X-ray diffraction (XRD) on the Bruker D8ADVANCE X-ray diffractometer at a voltage of 40 kV with Cu Kα radiation (λ=1.5406 Å) in the 2θ ranging from 10 to 80 degree. Scanning electron microscopy (S-4700, FE-SEM) with an acceleration voltage of 15 KV and transmission electron microscopy (TEM, Hitachi H-600-II, Japan) was conducted at 200 kV to characterize the morphology of PS-DVB/Fe_3O_4 and PFM. For TEM sample preparation, the products were dispersed in anhydrous ethanol by ultrasonication for 10 min and then fixed on a carbon-coated copper grid (FCF400-Cu). The magnetic properties were measured at room temperature using a BHV-55 vibrating sample magnetometer. The specific surface areas of TiO_2 samples were measured by nitrogen adsorption at 77.5 K (Micromeritics Tristar ASAP 2020) using Brunauer–Emmett–Teller (BET) method. Nitrate concentration was determined by the Shimadzu model ion chromatography equipment (IC).

3. Results and discussion

3.1 Characterization of PFM

To confirm the presence of crystalline magnetite within the polymer particles, the structure of the magnetic polymer particles was characterized by XRD. The XRD patterns of bare Fe_3O_4 nanoparticles, PS-DVB/Fe_3O_4 and PFM-3 particles were

illustrated in Fig.1, respectively. All the diffraction peaks match the six diffraction peaks well at (220), (311), (400), (422), (511) and (440) by comparing with Joint Committee on Powder Diffraction Standards (JCPDS card, file no. 79-0418), which were indexed to the cubic spinel phase of Fe_3O_4. The peak positions of Fe_3O_4 nanoparticles were unchanged before (black line) and after encapsulation by PS-DVB (red line), as well as functionalized by quaternary ammonium groups (blue line), which illustrated that the crystalline structure of Fe_3O_4 nanoparticles was not varied during the synthesis process of magnetic polymeric particles. In addition, the broad peak at about 18 degree might be due to the existence of PS-DVB (according to the red line) and PS-DVB with quaternary ammonium groups (according to the blue line).

Fig.2 showed the FT-IR spectra of pure Fe_3O_4, PS-DVB/Fe_3O_4 and PFM-3 particles. The adsorption peak at 583 cm^{-1} was the characteristic absorption of Fe-O bond which confirmed the presence of Fe_3O_4 nanoparticles. The peaks at 3038 cm^{-1} and 1597 cm^{-1} was corresponded to the stretching vibration of aromatic groups, the peak at 2925 cm^{-1} was corresponded to the methylene group, the three adsorption peaks at 1597, 1446 and 1500 cm^{-1} were due to the vibration of C-C bonds in the benzene ring, [32] which indicated the characteristic peaks of the PS-DVB according to the red line. Compared with the red line, a strong peak at 1114 cm^{-1} appeared according to the blue line, which was corresponded to the stretching vibration of the C-O-C group of polyelectrolytes.[34] The FTIR results thus suggested that polyelectrolyte chains were covalently grafted onto the PS-DVB/Fe_3O_4 microspheres.

The morphologies of PS-DVB/Fe_3O_4 microspheres were investigated by TEM

(ESI-1‡ (a)) and SEM (ESI-1‡ (b)), respectively. ESI-1‡ (a) showed a photograph of magnetic PS-DVB/Fe_3O_4 composite microspheres prepared by the method of magnetic colloid swelling polymerization after magnetic separation. It could be seen from the TEM images, these microspheres had excellent monodispersibility and all the composite particles were spherical in shape and the magnetite particles were encapsulated by PS-DVB. The average size of PS-DVB/Fe_3O_4 composite microspheres was approximate 0.7 μm. ESI-1‡ (b) showed a photograph of magnetic PS-DVB/Fe_3O_4 composite microspheres by SEM. Specifically, much wrinkled and rough topography presented on the surface of PS-DVB/Fe_3O_4 microspheres. It might be that some small size PS-DVB/Fe_3O_4 microspheres attached on the surface of the big ones. Although it may be not beautiful, it does increase the specific surface area. ESI-2‡ (a)-(c) showed the morphology of PFM-2 PFM-3 and PFM-4, respectively. The diameter of PFM was about 0.7μm, almost similar with PS-DVB/Fe_3O_4 microspheres. An interesting phenomenon was found by comparing these three images, the monodispersibility of PFM decreased with the increasing layer of quaternary ammonium groups, which might be due to the interaction between the quaternary ammonium groups.

The typical room-temperature magnetization curves of the bare Fe_3O_4 particles (Fig.3 (a)), oleic acid coated Fe_3O_4 particles (Fig.3 (b)), PS-DVB/Fe_3O_4 microspheres (Fig.3 (c)) and PFM-3 (Fig. 3 (d)) were recorded with VSM were illustrated in Fig. 3. As shown in the figure, the magnetization of the samples would approach the saturation values when the applied magnetic field between ±5000 Oe. Neither

remanence nor coercivity was observed, indicating that the magnetic particles produced were super paramagnetic and the single-domain magnetite nanoparticles remained in the polymer microspheres. The saturation magnetization of pure Fe_3O_4 nanoparticles, oleic acid coated Fe_3O_4 particles, PS-DVB/Fe_3O_4 microspheres and PFM-3 was about 66.9, 61.8, 36.4 and 29.1emu/g, respectively. The saturation magnetization of the nanoparticles was significantly less than that of bulk magnetite, which was 84emu/g.[35] The lower measured saturation magnetization could be due to the smaller size of the iron oxide nanoparticles and the low saturation magnetization of PS-DVB/Fe_3O_4 composite particles might be attributed to that Fe_3O_4 nanoparticles were wrapped up by polymer,[36] which added the thickness of polymer layer on the surface of the magnetite nanoparticles. The magnetic PS-DVB/Fe_3O_4 composite particles and PFM-3 can be separated from the aqueous solution under an external magnetic field, and could also be re-dispersed into the aqueous solution with agitation as shown in inset of Fig. 3. The magnetic PFM-3 aqueous solution was brown and homogeneous as shown in inset (b) of Fig.3. When the external magnetic field was applied, the PFM-3 was separated from the aqueous solution and the aqueous solution became clear as shown in inset (d) of Fig.3.

In the process of ion exchange, the specific surface area of the adsorbent would dominate a main effect. From BET adsorption isotherms, the specific surface area was calculated according to the method presented in literature and the data had been added in Table.1.[37] It was found that the specific surface area of the PFM decreased with the increasing of the layer of quaternary ammonium groups, and it may be due to the

interaction between the quaternary ammonium groups, which were consistent with the result of the SEM analysis.

3.2 Preparation process of PFM

The formation mechanism of PFM was described as schematically shown in ESI-3‡. Initially, magnetic Fe_3O_4 nanoparticles were synthesized by means of co-precipitation method and then the nanoparticles were modified by oleic acid, which led the nanoparticles became lipophilic. Secondly, the magnetic PS-DVB/Fe_3O_4 microspheres were prepared by the method of magnetic colloid swelling polymerization. In this process, the oleic acid coated PS-DVB/Fe_3O_4 could mix with the ST and DVB well to form small drops with the mechanical stirring, which was hydrophobic to the surrounding water phase. After the initiator being added into the solution the polymerization started and the PS-DVB/Fe_3O_4 was obtained. At last, the PS-DVB/Fe_3O_4 microspheres were functionalized by quaternary ammonium groups. To start the process, epoxy groups were introduced onto the surface of PS-DVB/Fe_3O_4 by modified with GMA. ESI-4‡ showed the following multi-step synthesis of PFM. In the step of (A), MA was reacted with epoxy groups by simple epoxy ring-opening reaction, and the secondary amine groups were obtained on the surface of PS-DVB/Fe_3O_4. Subsequently (B), a layer of cationic polyelectrolytes was formed by the reaction between the secondary amine groups and BDDE. Since the polyelectrolyte chain ends were terminated by glycidyl groups, secondary amine groups could be obtained on the surface of PS-DVB/Fe_3O_4 by another epoxy ring-opening reaction with MA (C). For the subsequent quaternization reaction, more

secondary amine groups were grafted onto the cationic polyelectrolytes. A defined number of bonded layers with desirable positive charge could be grafted onto the surface of PS-DVB/Fe_3O_4 by repeating the steps of (B) and (C) alternately.[34]

3.3 Equilibrium adsorption studies

Equilibrium adsorption isotherms of nitrate onto PFM were investigated. After adsorption experiment, the magnetic microsphere could be removed from water easily via introducing an external magnetic field and the separation method became easier than centrifugation. The amounts adsorbed at equilibrium (Q_e, mg/g) were further calculated by Eq. (1) .[38]

$$Q_e = \frac{V(C_0 - C_e)}{W} \quad (1)$$

Where C_0 and C_e are the concentrations of the nitrate in the solution at initial and equilibrium (mg/L), respectively; V is the volume of the solution (L); and W is the mass of the dry resin (g). As shown in Fig. 4, the adsorption capacity of PFM-3 resin was the highest (149.25 mg/g) compared with those of PFM-1 (79.77 mg/g), PFM-2 (124.62 mg/g) and PFM-4 (138.23 mg/g). The interesting thing was that the adsorption capacities of PFM-4 resins were lower than PFM-3, which was possibly due to that the specific surface area of the PFM decreased with the increasing of the layer of quaternary ammonium groups.

Nitrate adsorption isotherms onto NDP-2 resin were determined in the single-component solution and the experiment data were further correlated by the Langmuir (Eq. (2)) and Freundlich adsorption isotherm models (Eq. (3)).[1]

$$\frac{C_e}{Q_e} = \frac{1}{Q_0 b} + \frac{C_e}{Q_0} \quad (2)$$

$$Ln\mathrm{Q_e} = Ln\mathrm{K_f} + \frac{LnC_e}{\mathrm{n}} \quad (3)$$

where Q_0 is the maximum amount of nitrate adsorbed (mg/g); Q_e is the amount of nitrate adsorbed in equilibrium (mg/g); C_e is the nitrate concentration in equilibrium (mg/L); b is the Langmuir constants related to energy of adsorption; K_f and 1/n are Freundlich constants related to adsorption capacity and adsorption intensity, respectively. Fig. 5 showed that behavior of nitrate adsorption on PFM resin could be represented by Langmuir isotherm (Fig. 5a) and Freundlich isotherm (Fig. 5b) adsorption isotherm models well, and the regression coefficient (R_2) were ≥ 0.99. The Langmuir adsorption isotherm plots (Q_e vs. C_e) (Fig. 9a) and the Freundlich adsorption isotherm plots (Fig. 5b) showed the excellent applicability of Langmuir and Freundlich adsorption isotherms. The maximum capacity of PFM-3 resin was 149.25 mg/g, and energy of sorption value (b) is 0.090 L mg^{-1}. The results (Fig. 5 and Table 2) indicated that nitrate removal by PFM-3 performed best and could be represented by the Langmuir and Freundlich models reasonably. The major mechanism of sorption was electrostatic interaction and the using of large alkyl quaternary ammonium groups sacrifices the anion-exchange capacity due to a limited bead-surface area.[39, 40]

The pH of the aqueous solution was identified as one of the most important variable in the batch adsorption studies. The effect of different pH had been studied and the results were shown in Fig. 6a. Before the addition of the resin, the initial pH of solution was 6.24, and then solution pH was varied from 5 to 10 by adding 0.01 M HCl or 0.01 M NaOH. As depicted in Fig. 6a, the Q_e was very slight decrease for pH

varying from 5 to 10, which indicated that the considerable adsorption of nitrate independent of the pH for the PFM-3 resin. The final pH of the aqueous solution barely changed after the ion-exchange and removal of resin. The chloride ion on the PFM was exchanged by nitrate ion and the charge balance of the aqueous solution had not been broken. So the final pH of the aqueous solution did not change. Most attractively, at different locations where the pH of the water varied, the PFM-3 resin would exhibit almost the identical adsorption activity due to the independent of the pH. Considering the complex and variable polluted water system, the PFM-3 resin had broad prospects for practical application.

The reusability of ion exchange was one of the most important evaluation criterions. After adsorption experiment, the microspheres could be regenerated by ultrasonic washing with 0.6 M NaCl solution for three times and then dried in a vacuum oven. Fig.6b showed the reusability of PFM-3 under different concentrations of nitrate after different adsorbent cycles. We could see that the anion-exchange capacity slightly decreased in the first cycles and barely changed after the first cycle. The decrease in anion-exchange capacity was probably caused by residual nitrate in the pores of the microspheres. Excellent recycling property made PFM-3 microspheres potentially a cost-effective material.

4. Conclusion

A novel PFM-3 resin was synthesized successfully by a new magnetic colloid swelling polymerization method and following functioned by quaternary ammonium groups. The PFM-3 showed a higher adsorption capacity of nitrate (149.25 mg/g)

and exhibited almost the identical adsorption activity independent of the varied pH. In addition, these microspheres had shown excellent recycling property that they could keep good state even after being used repeatedly. Most importantly, this resin could be removed from solution easily via introducing an external magnetic field. So, it could be widely applied in purification of practical polluted drinking water resources in the near future.

Acknowledgments

This work was supported by the National Natural Science Foundation of China (NSFC, No.21246002), Technology Innovation Foundation of MOST (No. 11C26223204581), Natural Science Foundation of Jiangsu Prov. (No. BK2011328), 333 Talent project (2013) of Jiangsu Prov., and Minjiang Scholarship of Fujian Prov..

Notes and references

1 S.N. Milmile, J.V. Pande, S. Karmakar, A. Bansiwal, T. Chakrabarti and R.B. Biniwale, *Desalination*., 2011, **276** , 38-44.

2 P.K. Singh, S. Banerjee, A.L. Srivastava and Y.C. Sharma, *RSC Adv.*, 2015, **5**, 35365-35376.

3 J.B. Heredia, J.R. Domínguez, Y. Cano and I. Jime´nez, *Appl. Surf. Sci.,* 2006, **252**, 6031-6035.

4 A. Azizullah, M.N.K. Khattak, P. Richter, Häder and D.P. Azizullah, *Environ. Int.*, 2011, **37**, 479-497.

5 M.H. Ward and J.D. Brender, *Environ. Health.,* 2011, **4**, 167-178.

6 J.A. Camargo and Á. Alonso, *Environ. Int.*, 2006, **32**, 831-849.

7 J. Colman, G.E. Rice, J.M. Wright, E.S. Hunter, L.K. Teuschler, J.C. Lipscomb, R.C. Hertzberg, J.E. Simmons, M. Fransen, M. Osier and M.G. *Toxicol. Appl. Pharmacol.,* 2011, **254**, 100-126.

8 Y. Tong and Z. He, *RSC Adv.*, 2014, **4**, 10290-10294.

9 B. Basso and J.T. Ritchie, *Agric. Ecosyst. Environ.*, 2005, **108**, 329-341.

10 M. Maeda, B. Zhao, Y. Ozaki and T. Yoneyama, *Environ. Pollut.,* 2003, **121**, 477-487.

11 N. Mehrabi, M. Soleimani, M.M. Yeganeh and H. Sharififard, *RSC Adv.,* 2015, **5**, 51470-51482.

12 S.P. Suriyaraj, M.M. Pillai, A. Bhattacharyya and R. Selvakumar, *RSC Adv.*, 2015, **5**, 68420-68429.

13 M. Boumediene and D. Achour, *Desalination.,* 2004, **168,** 187-194.

14 L. Yuan and T. Kusuda, *J. Appl. Polym. Sci.,* 2005, **96**, 2367-2372.

15 H. Jiang, P. Chen, S. Luo, X. Tu, Q. Cao and M. Shu, *Appl. Surf. Sci.*, 2013, **284**, 942-949.

16 A. Mautner, H.A. Maples, H. Sehaqui T. Zimmermann, U.P. Larraya, A.P. Mathew, C.Y. Lai, K. Lif and A. Bismarckand, *Environ. Sci.: Water Res. Technol.*, 2015, DOI: 10.1039/c5ew00139k.

17 A. Bhatnagar and M. Sillanpää, *Chem. Eng. J.,* 2011, **168,** 493-504.

18 S.K. Nataraj, K.M. Hosamani and T.M. Aminabhavi, *J. Appl. Polym. Sci.,* 2006, **99**, 1788-1794.

19 Z.L. Feng, W.R. Wei, L.T. Wang and R.Y. Hong, *Appl. Surf. Sci.*, 2015, **357**, 759-765.

20 H. Song, Y. Zhou, A. Li and S. Mueller, *Desalination.,* 2012, **296**, 53-60.

21 H. Yan, L. Yang, Z. Yang, H. Yang, A. Li and R. Cheng, *J. Hazard. Mater.,* 2012, **229,** 371-380.

22 S. Zhang, Y. Zhang, G. Bi, J. Liu, Z. Wang, Q. Xu, H. Xu and X. Li, *J. Hazard. Mater.*, 2014, **27**, 27-34.

23 Z. Hua, B. Yang, W. Chen, X. Bai, Q. Xu and H. Gu, *Appl. Surf. Sci.,* 2014, **317**, 226-235.

24 E.T. Ozer, B. Osman, A. Kara, N. Besirli, S. Gucer and H. Sozeri, *J. Hazard. Mater.*, 2012, **229**, 20-28.

25 H.Y. Zhu, R. Jiang, L. Xiao and W. Li, *J. Hazard. Mater.*, 2010, **179**, 251-257.

26 Q. Liu, L. Wang, A. Xiao, J. Gao, W. Ding, H. Yu, J. Huo and M. Ericson, *J. Hazard. Mater.,* 2010, **181**, 586-592.

27 Y. Tai, L. Wang, J. Gao, W.A. Amer, W. Ding and H. Yu, *J. Colloid Interface Sci.,* 2011, **360**, 731-738.

28 A. Pavıa-Sanders, S. Zhang, J.A. Flores and K.L. Wooley, *ACS Nano.,* 2013, **7,** 7552-7561.

29 Q. Zhu, F. Tao and Q. Pan, *ACS Appl. Mater. Interfaces.,* 2010, **2**, 3141-3146.

30 L. Zhu, C. Li, J. Wang, H. Zhang, J. Zhang, Y. Shen, C. Li, C. Wang and A. Xie, *Appl. Surf. Sci.,* 2012, **258**, 6326-6330.

31 M. Chen, W. Jiang, F. Wang, P. Shen, P. Ma, J. Gu, J. Mao and F. Li, *Appl. Surf.*

Sci., 2013, **286**, 249-256.

32 J. Mao, W. Jiang, J. Gu, S. Zhou, Y. Lu and T. Xie, *Appl. Surf. Sci.,* 2014, **317**, 787-793.

33 X. Liu, H. Liu, J. Xing, Y. Guan, Z. Ma, G. Shan and C. Yang, *China Particuology.*, 2003, **1**, 76-79.

34 Y.L. Chen, B.C. Pan, H.Y. Li, W.M. Zhang, L. Lv and J. Wu, *Sci. Technol.,* 2010, **44,** 3508-3513.

35 Z. Huang, L. Xi, Q. Subhani, W.bYan, W. Guo and Y. Zhu, *Carbon.,* 2013, **62,** 127-134.

36 M. Yamaura, R.L. Camilo, L.C. Sampaio, M.A. Macêdo, M. Nakamura and H.E. Toma, *J. Magn. Magn. Mater.,* 2004, **279**, 210-217.

37 Y. Chen, Z. Qian and Z.C. Zhang, *Colloid Surf. A.,* 2008, **312**, 209-213.

38 K.S.W. Sing, *Pure Appl Chem.*, 1985, **57**, 603-619.

39 J.N. Wang, Y. Zhou, A.M. Li and L. Xu, *J. Hazard. Mater.*, 2010, **176**, 1018-1026.

40 B.H. Gu, Y.K. Ku and P.M. Jardine, *Sci. Technol.*, 2004, **38**, 3184-3188.

Figure captions

Fig.1: XRD diffraction pattern of (a) oleic acid coated Fe_3O_4 nanoparticles, (b) PS-DVB/Fe_3O_4, (c) PFM-3.

Fig.2: FTIR spectra of pure Fe_3O_4 (black line), PS-DVB/ Fe_3O_4 (red line), PFM-3 (blue line).

Fig.3: Room temperature magnetization curves of (a) pure Fe_3O_4 nanoparticles, (b) oleic acid coated Fe_3O_4 nanoparticles, (c) PS-DVB/Fe_3O_4 microspheres, (d) PFM-3. The inset showed the digital photographs of (a) pure Fe_3O_4 nanoparticles and (b) PFM-3 were separated from deionized water.

Fig.4: Equilibrium adsorption isotherms of nitrate on PFM-1, PFM-2, PFM-3 and PFM-4 from model solutions at 293 K.

Fig.5: (a) Equilibrium Langmuir isotherm and (b) Freundlich isotherm for nitrate adsorbed using PFM-1, PFM-2, PFM-3 and PFM-4.

Fig.6: (a) Effect of varied PH on anion-exchange capacity of PFM-3. (b) Anion-exchange capacity of PFM-3 after different anion-exchange cycles.

Table captions

Table.1: Properties of PFMs.

Table.2: Values of the parameters for nitrate from water onto different adsorbents at 293 K as obtained from the (a) Langmuir and (b) Freundlich equation.

bGraphical abstract: Schematic of the formation process of PFM.

Property	BET surface area (m^2/g)	Micropore area (m^2/g)	Average pore diameter (nm)	Pore volume (ml/g)
PMF-1	34.58	3.21	9.32	0.084
PMF-2	29.27	2.54	8.54	0.075
PMF-3	23.56	2.16	6.97	0.063
PMF-4	15.41	1.27	5.02	0.042

Table.1.Properties of the PMF.

Adsorbent	Langmuir equation			Freundlich equation		
	Q_0(mg/g-dry resin)	b (L/mg)	R^2	n	K_f (mg/g)	R^2
PFM-1	82.51	0.056	0.999	3.17	14.90	0.992
PFM-2	130.04	0.046	0.994	2.90	18.13	0.996
PFM-3	149.25	0.090	0.993	3.48	31.85	0.995
PFM-4	141.84	0.073	0.995	3.28	27.51	0.974

Table.2.Values of the parameters for nitrate from water onto different adsorbents at 293 K as obtained from the Langmuir and Freundlich equation.

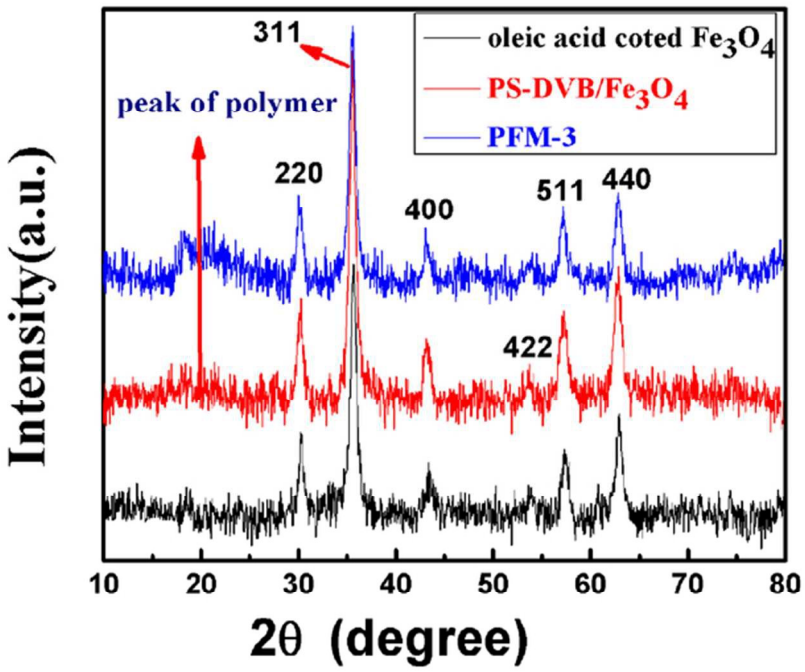

64x49mm (300 x 300 DPI)

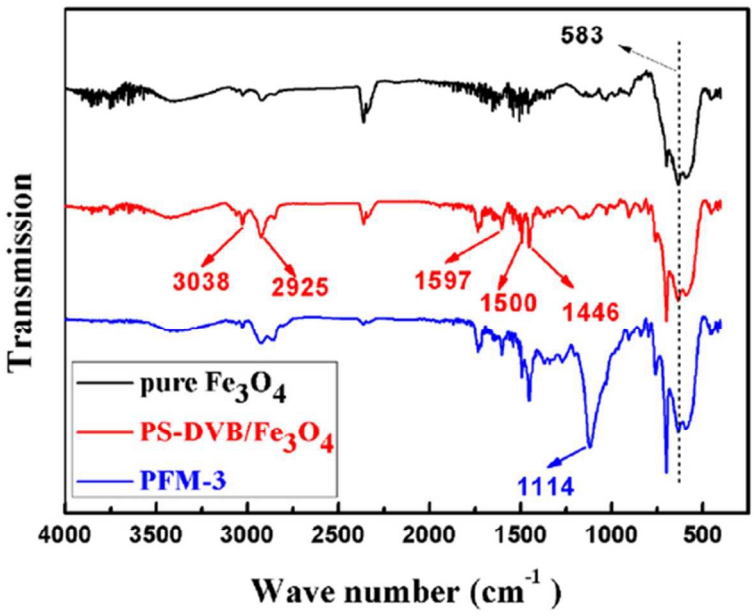

58x40mm (300 x 300 DPI)

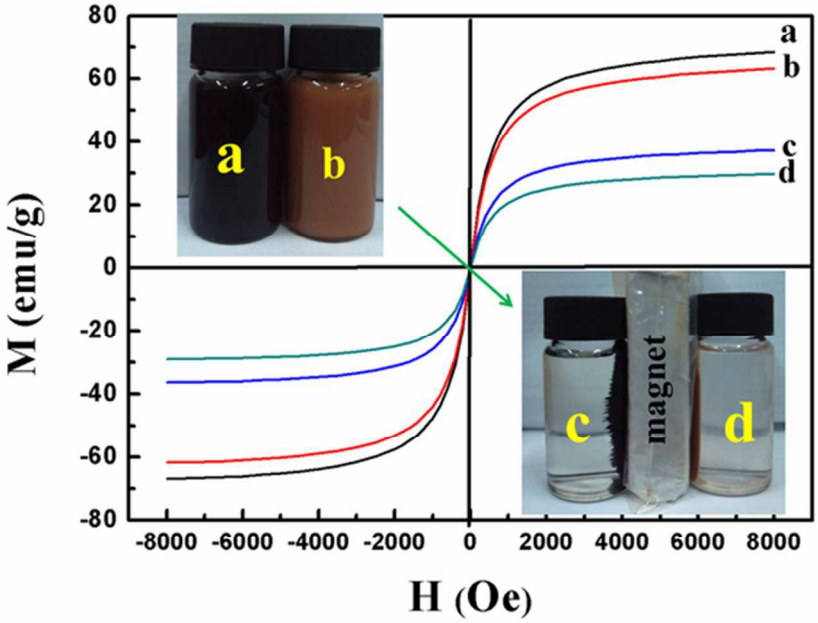

58x40mm (300 x 300 DPI)

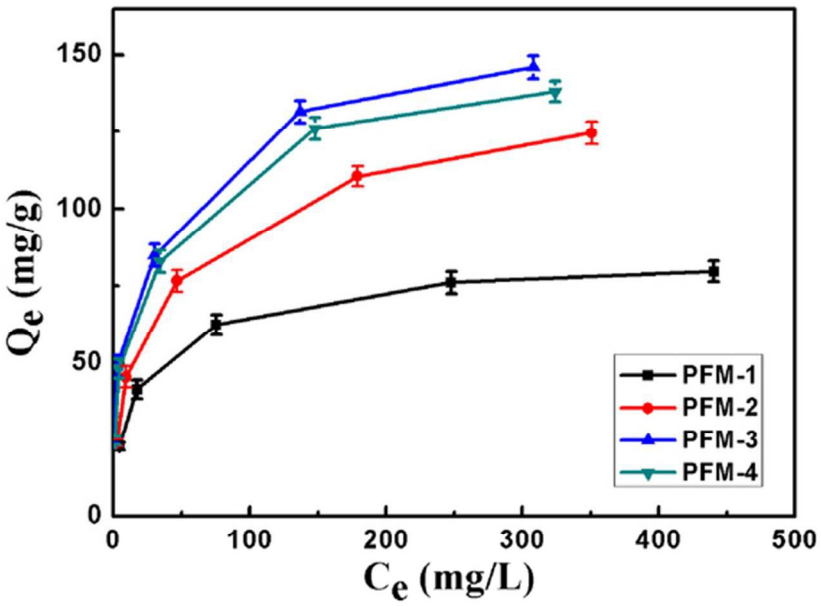

58x41mm (300 x 300 DPI)

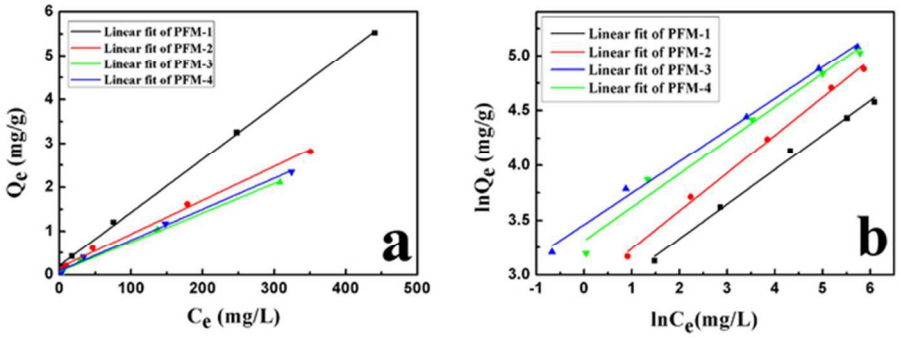

62x23mm (300 x 300 DPI)

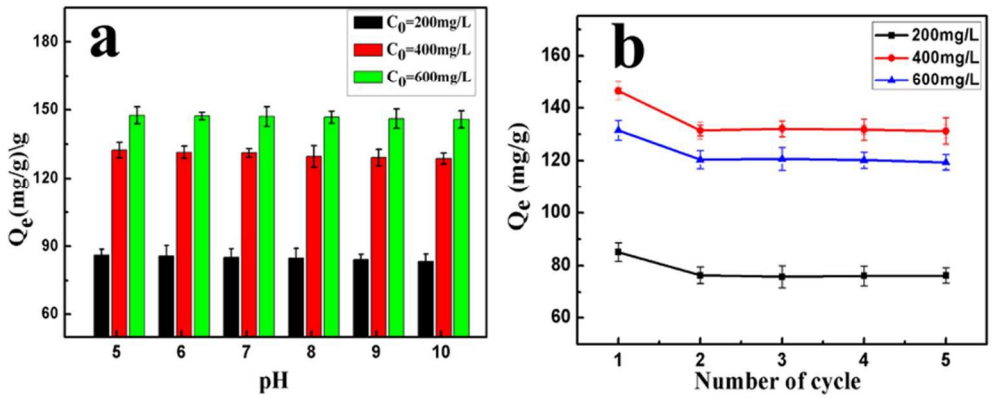

73x31mm (300 x 300 DPI)